Supplementary information:

Shifts in ecosystem equilibria following trophic rewilding

Authors: Selwyn Hoeks[1]*, Mark A.J. Huijbregts[1], Coline C.F. Boonman[2], Søren Faurby[3], Jens-C. Svenning[2], Michael B.J. Harfoot[4, 5], Luca Santini[6].

[1]Department of Environmental Science, Radboud Institute for Biological and Environmental Sciences (RIBES), Radboud University, The Netherlands.

[2]Center for Biodiversity Dynamics in a Changing World (BIOCHANGE) and Section for Ecoinformatics and Biodiversity, Department of Biology, Aarhus University, Denmark.

[3]Department of Biological and Environmental Sciences, University of Gothenburg, Göteborg, Sweden.

[4]United Nations Environment World Conservation Monitoring Centre, United Kingdom

[5]Vizzuality, Calle de Fuencarral, 123, 28010, Madrid, Spain

[6]Department of Biology and Biotechnologies "Charles Darwin", Sapienza University of Rome, Rome, Italy

*corresponding author: s.hoeks@science.ru.nl

Text S1: R-package modifications

To improve the realism of our simulations we made two modifications to the original R package (Hoeks et al., 2021). The modified package version can be found at: https://anonymous.4open.science/r/RewildMadingleyR-FCC9/.

First, the Madingley assumes one single vegetation stock on which herbivores depend on and compete for (Harfoot et al., 2014). This can result in unrealistic outcomes when certain herbivore guilds are taken out of the simulation. To release the unrealistic assumption of competition between small and large herbivores (or omnivores) all herbivore and omnivore cohorts were assigned to eight bins using adult body mass and $\log_{10}$ breaks. The vegetation mass was separated over eight equal proportions at the start of the simulation. Each proportion of vegetation biomass was assigned to a specific herbivore bin. Vegetation growth was simulated by dividing the default growth equally over the eight vegetation proportions. This assumption is based on the energy-equivalence rule, which assume that energy in ecosystems is distributed independently of the size of organisms (Brown et al., 2004). Despite many studies have challenged this theory (Carbone et al., 2007; Isaac et al., 2011, 2013; Pedersen et al. 2017; Santini et al. 2021), Hatton et al. (2019) have recently shown the pattern holds when investigated across a large range of organisms, which suggests it can be an acceptable approximation for a global ecosystem model.

Second, preliminary tests highlighted an unexpected outcome. The removal of large-bodied mammals led to an increase in mesocarnivores and omnivores, which in turn increased their consumption on small-bodied endothermic cohorts driving them to extinction. While an increase in mesocarnivores and omnivores and consequent impact on small herbivores is possible (Roemer et al., 2009; Moreno-Opo et al., 2015), a complete eradication of all small-bodied species is unlikely. In fact, while in the Madingley no heterogeneity in the landscape exists, in reality small species can persist in areas that are inaccessible to larger species. To avoid this, we set a density threshold below which it becomes impossible for a predator to prey on a target cohort. This basically assumes that predation on a given prey becomes very unlikely when this is rare. We assumed that

endotherms with a body mass <150g that reach a density of <1 individual per km^2 become invisible to predators. This is a highly conservative assumption, as small mammals <150g generally occur at very high densities (Santini et al. 2022).

Table S1. Functional properties used for the initialization of cohorts.

Functional group	Feeding mode	Reproductive strategy	Thermo-regulation mode	Maximum mass (kg)	Herbivore assimilation efficiency (%)	Carnivore assimilation efficiency (%)
1	Herbivore	Iteroparity	Endotherm	700	50	80
2	Carnivore	Iteroparity	Endotherm	50	0	0
3	Omnivore	Iteroparity	Endotherm	200	40	64
4	Herbivore	Semelparity	Ectotherm	0.02	50	80
5	Carnivore	Semelparity	Ectotherm	0.02	0	0
6	Omnivore	Semelparity	Ectotherm	0.02	40	64
7	Herbivore	Iteroparity	Ectotherm	1.5	50	80
8	Carnivore	Iteroparity	Ectotherm	10	0	0
9	Omnivore	Iteroparity	Ectotherm	0.2	40	64

Table S2. Trait-based community dissimilarity and the additive components 'turnover' and 'nestedness', comparing the maximum trait space volume of the initial and post reintroduction state. The dissimilarity in maximum trait space volume was calculated using the *mFD* package (Magneville et al., 2022) and comprised of three traits: 1) $\log_{10}$ adult body mass, 2) the functional group index (see Table S1), and 3) the trophic level. Jaccard indices are presented as mean values computed across 10 simulation replicates. Standard deviations are shown in brackets.

Reintroduction scenario	Location	Jaccard (%)	Turnover (%)	Nestedness (%)
Main scenario: Herbivores + omnivores + delayed carnivore reintroduction	High NPP – Low Seasonality	8.37 (1.17)	3.66 (2.01)	4.71 (2.13)
	High NPP – High Seasonality	9.21 (3.76)	1.16 (0.36)	8.05 (2.23)
	Low NPP – Low Seasonality	10.32 (3.11)	5.11 (1.07)	5.21 (0.89)
	Low NPP – High Seasonality	8.42 (3.31)	0.49 (0.27)	7.91 (2.41)
Alternative scenario 1: Herbivores + omnivores + carnivores (reintroduced during one phase)	High NPP – Low Seasonality	7.62 (3.01)	3.57 (1.97)	4.05 (3.43)
	High NPP – High Seasonality	8.23 (2.37)	2.13 (1.40)	6.12 (1.11)
	Low NPP – Low Seasonality	11.11 (2.84)	6.44 (3.51)	4.67 (3.34)
	Low NPP – High Seasonality	8.13 (2.52)	3.94 (2.77)	4.19 (2.48)
Alternative scenario 2: Herbivores + omnivores (no carnivores)	High NPP – Low Seasonality	11.21 (1.52)	5.56 (4.09)	5.65 (3.70)
	High NPP – High Seasonality	14.51 (2.02)	4.34 (2.25)	10.16 (3.71)
	Low NPP – Low Seasonality	12.57 (2.80)	4.06 (3.09)	8.51 (3.19)
	Low NPP – High Seasonality	16.48 (4.65)	5.63 (3.38)	10.85 (3.78)

Table S3. Jaccard indices quantifying the overall biomass distribution dissimilarity. Because the Madingley model follows a trait-based approach (i.e. does not model species) and traits are modeled on a continues scale, grouping cohorts into larger aggregates is required for the comparison of two communities using the regular Jaccard index. We aggregated the biomass of cohorts using $\log_{10}$ body mass bins and functional group (see Table S1). The resulting bins were used to calculate the Jaccard index using the 'vegdist' function of the *vegan* package (Oksanen et al., 2007). Jaccard indices are presented as mean values computed across 10 simulation replicates. Standard deviations are shown in brackets.

Reintroduction scenario	Location	Jaccard (%)
Main scenario: Herbivores + omnivores + delayed carnivore reintroduction	High NPP – Low Seasonality	27.0 (5.04)
	High NPP – High Seasonality	29.7 (5.42)
	Low NPP – Low Seasonality	25.2 (2.75)
	Low NPP – High Seasonality	31.3 (8.35)
Alternative scenario 1: Herbivores + omnivores + carnivores (reintroduced during one phase)	High NPP – Low Seasonality	22.4 (4.67)
	High NPP – High Seasonality	22.1 (3.13)
	Low NPP – Low Seasonality	20.1 (4.45)
	Low NPP – High Seasonality	25.5 (3.19)
Alternative scenario 2: Herbivores + omnivores (no carnivores)	High NPP – Low Seasonality	38.5 (6.35)
	High NPP – High Seasonality	36.0 (6.17)
	Low NPP – Low Seasonality	38.1 (3.85)
	Low NPP – High Seasonality	35.6 (4.13)

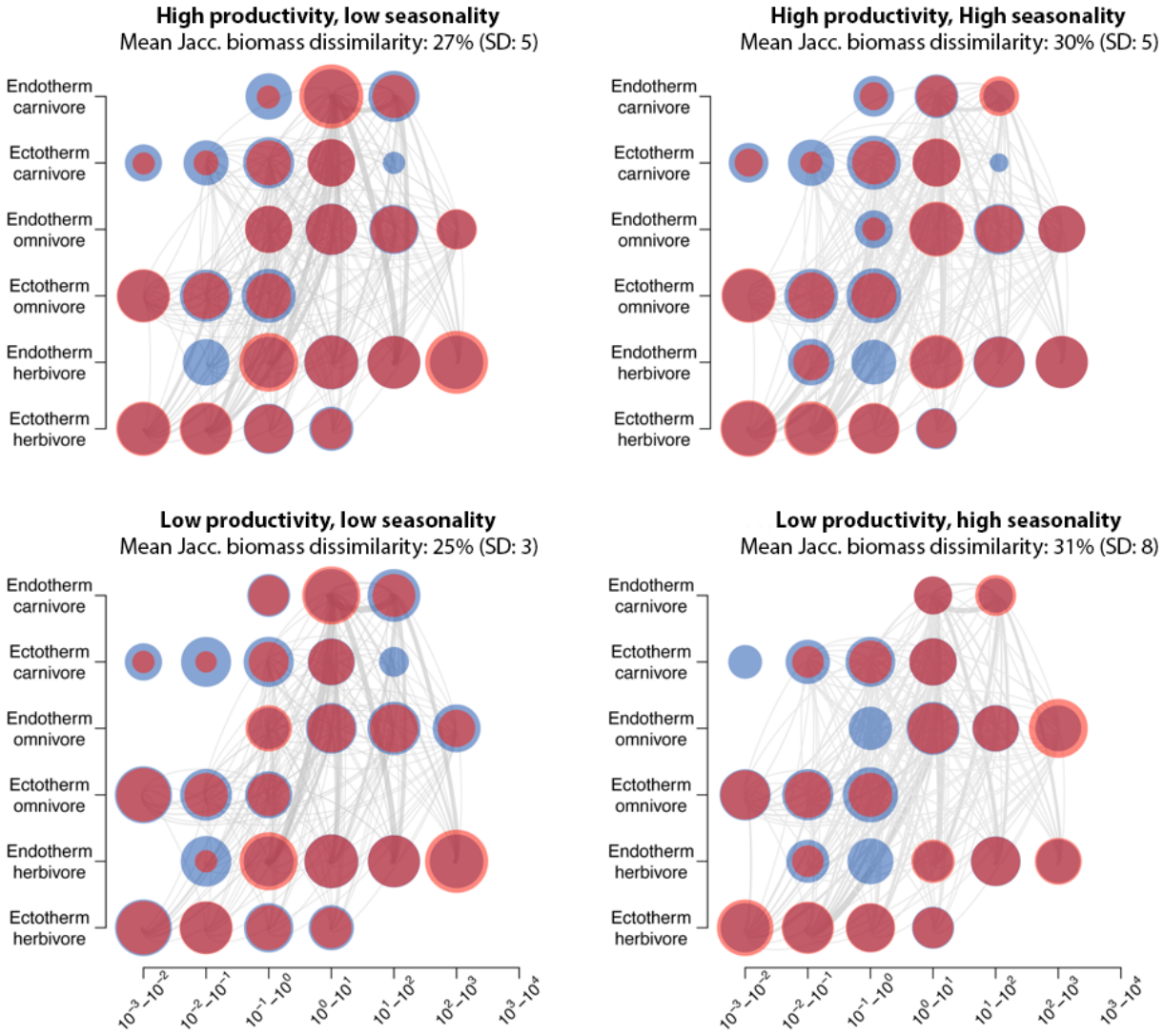

Fig. S1 Food-web plots from the initial state compared to the post reintroduction state for the main reintroduction scenario. Large-bodied endothermic cohorts were removed from the initial state, starting from the heaviest. After the model reached equilibrium, large herbivores and large omnivores were reintroduced, followed by a delayed reintroduction of large carnivores. Blue circles in the food-web plots depict the absolute $\log_{10}$ biomass found in the initial state. Red circles in the food-web plots depict the absolute $\log_{10}$ biomass observed in the post-reintroduction state. Biomass distribution Jaccard dissimilarity indices were calculated by summing the biomass of cohorts within the same $\log_{10}$ body mass bin and same functional group and comparing these aggregates from the initial to those of the post-reintroduction state. Jaccard indices were calculated using the 'vegtdist' fuction of the *vegan* package (Oksanen et al., 2007) Jaccard indices shown here represent the mean and standard deviation (denoted as SD) computed across 10 replicates.

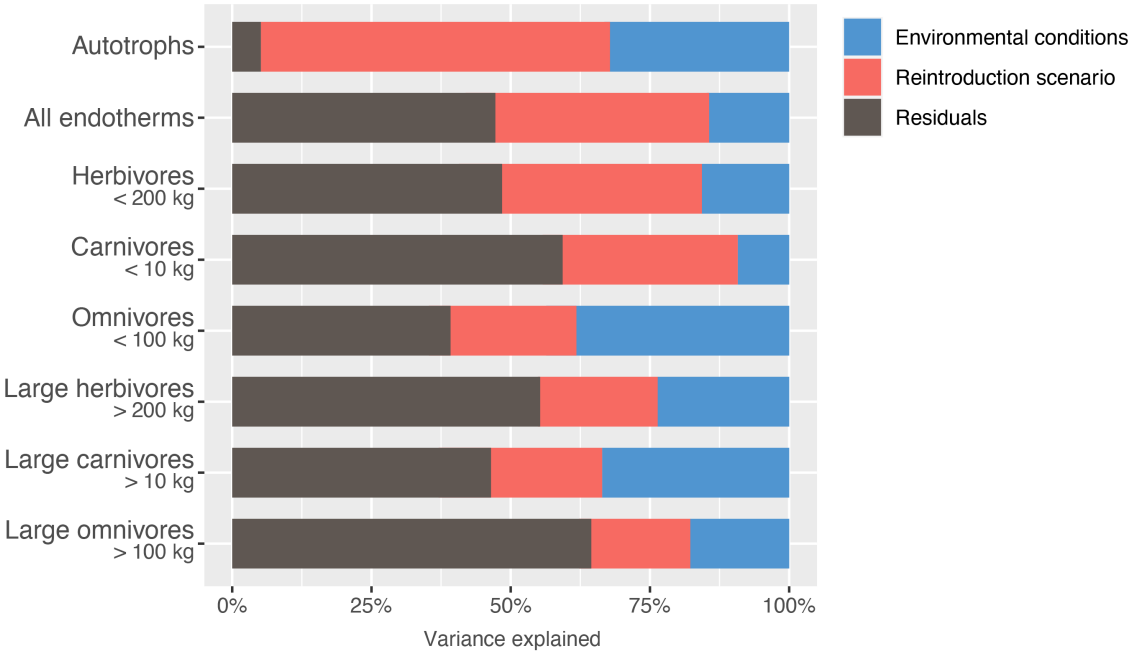

Fig. S2 Variance decomposition analysis, excluding results from alternative reintroduction scenario 2. Contribution of local environmental conditions and different reintroduction scenarios to the variance in simulated response ratios. This figure only include the variation in response ratios for the main reintroduction scenario (where large herbivores (> 200 kg) and omnivores (> 100 kg) are reintroduced first, followed by the reintroduction of large carnivores (> 10 kg) in a second reintroduction phase) and the variation in response ratios for alternative reintroduction scenario 1 (reintroduction of all large mammal cohorts in one single phase). The response ratio was calculated by taking the natural logarithm of the biomass in the post-reintroduction state divided by the biomass in the initial state. Biomass inputs used to derive the response ratios were based on yearly averages computed over the last 5 years of the simulation phase. The variance explained was calculated using an ANOVA, in which the sum of squares for the reintroduction scenario, the local environmental conditions, as well as the residuals was divided by the total sum of squares. The variance decomposition analysis includes results from 10 simulation replicates per unique combination of reintroduction scenarios and local environmental conditions.

References

Brown, J. H., Gillooly, J. F., Allen, A. P., Savage, V. M., & West, G. B. (2004). Toward a metabolic theory of ecology. Ecology, 85(7), 1771-1789.

Carbone, C., Rowcliffe, J. M., Cowlishaw, G., & Isaac, N. J. (2007). The scaling of abundance in consumers and their resources: implications for the energy equivalence rule. The American Naturalist, 170(3), 479-484.

Hatton, I. A., Dobson, A. P., Storch, D., Galbraith, E. D., & Loreau, M. (2019). Linking scaling laws across eukaryotes. Proceedings of the National Academy of Sciences, 116(43), 21616-21622.

Harfoot, M. B., Newbold, T., Tittensor, D. P., Emmott, S., Hutton, J., Lyutsarev, V., ... & Purves, D. W. (2014). Emergent global patterns of ecosystem structure and function from a mechanistic general ecosystem model. PLoS biology, 12(4), e1001841.

Hoeks, S., Tucker, M. A., Huijbregts, M. A., Harfoot, M. B., Bithell, M., & Santini, L. (2021). MadingleyR: An R package for mechanistic ecosystem modelling. Global Ecology and Biogeography, 30(9), 1922-1933.

Isaac, N. J., Storch, D., & Carbone, C. (2011). Taxonomic variation in size–density relationships challenges the notion of energy equivalence. Biology Letters, 7(4), 615-618.

Isaac, N. J., Storch, D., & Carbone, C. (2013). The paradox of energy equivalence. Global Ecology and Biogeography, 22(1), 1-5.

Magneville, C., Loiseau, N., Albouy, C., Casajus, N., Claverie, T., Escalas, A., ... & Villéger, S. (2022). mFD: an R package to compute and illustrate the multiple facets of functional diversity. Ecography, 2022(1).

Moreno-Opo, R., Afonso, I., Jiménez, J., Fernández-Olalla, M., Canut, J., García-Ferré, D., ... & López-Bao, J. V. (2015). Is it necessary managing carnivores to reverse the decline of endangered prey species? Insights from a removal experiment of mesocarnivores to benefit demographic parameters of the Pyrenean capercaillie. PLoS One, 10(10), e0139837.

Oksanen, J., Kindt, R., Legendre, P., O'Hara, B., Stevens, M. H. H., Oksanen, M. J., & Suggests, M. A. S. S. (2007). The vegan package. Community ecology package, 10(631-637), 719.

Pedersen, R. Ø., Faurby, S., & Svenning, J. C. (2017). Shallow size–density relations within mammal clades suggest greater intra-guild ecological impact of large-bodied species. Journal of Animal Ecology, 86(5), 1205-1213.

Roemer, G. W., Gompper, M. E., & Van Valkenburgh, B. (2009). The ecological role of the mammalian mesocarnivore. BioScience, 59(2), 165-173.

Santini, L., & Isaac, N. J. (2021). Rapid Anthropocene realignment of allometric scaling rules. Ecology Letters, 24(7), 1318-1327.

Santini, L., Benítez-López, A., Dormann, C. F., & Huijbregts, M. A. (2022). Population density estimates for terrestrial mammal species. Global Ecology and Biogeography, 31(5), 978-994.

139 Smith, M. J., Purves, D. W., Vanderwel, M. C., Lyutsarev, V., & Emmott, S. (2013). The climate
140 dependence of the terrestrial carbon cycle, including parameter and structural uncertainties.
141 Biogeosciences, 10(1), 583-606.